East European Journal of Physics. 3. 4-16 (2025)
DOI:10.26565/2312-4334-2025-3-01 ISSN 2312-4334

CONSTRAINED DYNAMICS OF HOLOGRAPHIC DARK ENERGY IN MODIFIED $f(R)$ GRAVITY

A.Y. Shaikh[a#], A.P. Jenekar[b†], S.M. Shingne[c*]
[a]*Department of Mathematics, Indira Gandhi Kala Mahavidyalaya, Ralegaon-445402, (M.S.) India*
[b]*Department of Mathematics, Arts, Commerce and Science College, Maregaon-445303, (M.S.) India*
[c]*Department of Mathematics, G. S. Science, Arts and Commerce College, Khamgaon-444312, (M.S.) India*
**Corresponding Author E-mail: smshingne131@gmail.com*; [#]*E-mail: shaikh_2324ay@yahoo.com*; [†]*E-mail: apjenekar@gmail.com*
Received May 21, 2025; revised July 8, 2025; accepted July 13, 2025

In the present work, we examine the dynamical behaviour of holographic dark energy (HDE) within the framework of modified $f(R)$ gravity in a hypersurface-homogeneous space-time. To explore the universe's evolutionary behaviour under the influence of dark energy, we consider both exponential and power-law expansions. The cosmic evolution is analysed using standard cosmological diagnostics, including the density parameter and equation of state (EoS) parameter along with the deceleration parameter. Furthermore, the statefinder diagnostic pair is tested to detect precisely different phases of the universe. The squared speed of sound parameter was used to incorporate the stability analysis for our models. This investigation links the principles of quantum gravity to cosmology, producing testable predictions for forthcoming research and illustrating that HDE functions as a credible alternative to ΛCDM.
Keywords: *Hypersurface-homogeneous space time; f(R) gravity; Holographic dark energy*
PACS: 98.80.−k, 04.50.Kd, 95.36.+x

1. INTRODUCTION

The revelation of cosmic acceleration was a game-changing discovery in the history of cosmology. The initial detection occurred through the observation of Type Ia supernovae by Riess et al. [1-3], also analysed through Cosmic Microwave Background Radiation (CMBR) [4]. This discovery totally changed how we see the universe. It showed that the rate of expansion is getting faster, which goes against what we thought matter-dominated Friedmann model predictions were. These groundbreaking findings showed that the cosmos is actually expanding at a faster rate than it previously was thought, which totally changes what we know about how the cosmos works. The recently discovered measurements carried out by means of Type Ia supernovae match the precision of standard candles, demonstrating that distant supernovae appeared fainter than expected in a decelerating universe, strongly suggesting the presence of a mysterious repulsive force counteracting gravitational attraction on cosmological scales. We now have a lot of evidence which shows that our universe is expanding faster and faster, where dark energy is the main source causing it. We have got different probes that include precision observations of CMB anisotropies by WMAP and Planck [5], which measure the detailed mapping of baryon acoustic oscillations (BAO) [6] and comprehensive large-scale structure surveys [7], which have established beyond reasonable doubt that we live in an accelerating universe dominated by what we now call dark energy. All of the available evidence shows that dark energy – an enigmatic component constituting approximately a whopping 68% of the universe's energy –exhibits negative pressure characteristics.

The simplest theoretical framework that explains these observations is the ΛCDM model. This model adds Einstein's cosmological constant, represented with Λ into the field equations of general relativity (GR) to represent a constant vacuum energy density that fills all of space. This standard model has been successful in the fitting of observational data; however, it is confronted by two significant challenges. Firstly, the significant difference between the predicted values from quantum field theory and the observed value of the cosmological constant leads to the fine-tuning concern [8-11]; and second, the coincidence problem asks why dark energy became dynamically important only recently in cosmic history, at the special epoch when human observers happen to exist [12]. These basic issues have led cosmologists to check out dynamical dark energy models where the energy density evolves with time and remains constant. Out of these most interesting options, that holographic dark energy (HDE) is emerging as one of the most compelling alternatives that relies on quantum gravity's holographic principle [13-16].

The HDE framework is based on some interesting ideas from black hole thermodynamics and string theory. It proposes that the amount of dark energy density in a given volume is fundamentally limited by the amount of information allowed to boundthe volume's boundary, leading to the characteristic relation $\rho_{de}=3c^2M_p^2L^{-2}$ [17], where represents an infrared cutoff scale that is identified with the future event horizon. This elegant formulation naturally sidesteps the fine-tuning problem because of its inherent scale dependence and provides a dynamical equation of state that may resolve the coincidence problem while maintaining a deep connection to fundamental quantum gravitational principles. Pawar et al. [18] recent work has shown the advantages of this in anisotropic cosmological settings and how the holographic approach works even in generalised spacetime geometries. However, when the HDE model is implemented within general relativity, these models

Cite as: A.Y. Shaikh, A.P. Jenekar, S.M. Shingne, East Eur. J. Phys. 3, 4 (2025), https://doi.org/10.26565/2312-4334-2025-3-01

also encounter difficulties in simultaneously describing both the early inflationary epoch and late-time acceleration [19-20], limitations that have prompted investigation and study of generalised versions of the Einstein-Hilbert interaction for modified gravity to include additional curvature-dependent terms. Buchdahl [21] introduced $f(R)$ gravity as a generalisation of Einstein's relativity, whereas Starobinsky gravity $f(R)=R+\alpha R^{l}$ [22] is the most motivated modification, which is an exhilaratingly innovative theory of gravity that introduces a quadratic curvature correction to the Einstein-Hilbert action. It was among the first and most successful models of cosmic inflation, providing a purely geometric explanation for the exponential expansion of the early universe without requiring additional scalar fields. This theory was originally proposed to explain inflation through the dominant effects of the term at high curvatures and subsequently shown to produce inflationary predictions in excellent agreement with precision CMB measurements from Planck [23], while it might play a role in contributing to late-time acceleration through its curvature effects.

To fully explore what happens when the cosmological implications combine holographic dark energy with modified gravity, it is essential to move beyond the restrictive assumption of perfect isotropy inherent in the standard Friedmann-Lemaître-Robertson-Walker metric. Instead, we should explore a more general geometrical structure that maintains spatial homogeneity while allowing for anisotropic expansion effects, meaning allowing for different rates of expansion along different spatial directions. Hypersurface-homogeneous spacetimes [24-30] provide such a framework, offering a richer dynamical context for investigating dark energy that is particularly relevant for understanding the early universe before inflation erased primordial anisotropies [31,32], as well as for probing potential connections between the presence of dark energy followed by the formation of immense structures [33]. In this study, we examine holographic dark energy within the $f(R)$ gravity framework using a hypersurface-homogeneous spacetime background. We come up to deriving exact solutions for both exponential $\left(a(t)\sim e^{nt}\right)$ and power-law $\left(a(t)\sim t^{m}\right)$ expansion scenarios. These represent idealized cases of inflationary and late-time acceleration respectively. Through detailed analysis of key cosmological parameters including the evolution of density components $\Omega_i(z)$ [34-36], the dynamical equation of state $\omega(z)$ [37-39], the deceleration parameter $q(z)$ with statefinder diagnostics $\{r,s\}$ [40], while carefully tracking the development of anisotropy through the shear scalar σ^2, we have demonstrate several significant results: the model naturally produces accelerated expansion without fine-tuning. It also shown an asymptotic approach to a cosmological constant-like equation of state $(\omega=-1)$ at late times, and shows anisotropy evolution patterns consistent with current observational constraints from the CMB. These findings suggest that the synthesis of HDE with $f(R)$ gravity in an anisotropic cosmological framework may provide a more comprehensive and theoretically satisfying description of cosmic acceleration that addresses fundamental limitations of the standard ΛCDM model [41] while maintaining consistency with current observational evidence. Furthermore, this approach offers new insights into the deep connection between quantum gravity, modified gravity, and dark energy [42, 43], while making specific predictions that can be tested with next-generation cosmological surveys.

This motivates us to consider volumetric expansion of the exponential, and power-law kinds to examine the $f(R)$ gravity-based HDE within hypersurface-homogeneous space-time. The paper is structured as follows. Section 2 examines cosmology in considered space-time by integrating the HDE model with pressureless dark matter. The quadrature solutions for scale factors in field equations are contained in section 3. The physical and kinematical characteristics of our volumetric expansion models are explored in sections 4 and 5, whereas section 6 offers statefinder diagnostics along with the model's stability analysis. Section 7 concludes with a discussion of the results.

2. METRIC AND FIELD EQUATIONS

The action for $f(R)$ gravity is expressed as

$$S=\int\sqrt{-g}\left(f(R)+L_m\right)d^4x, \tag{1}$$

where $f(R)$ serves as a general function of the Ricci scalar R and L_m stands for the usual matter Lagrangian.

The field equations can be derived by varying the action pertaining to the metric $g_{\mu\nu}$ as

$$F(R)R_{\mu\nu}-\frac{1}{2}f(R)g_{\mu\nu}-\nabla_\mu\nabla_\nu F(R)+g_{\mu\nu}\nabla^\mu\nabla_\mu F(R)=-(T_{\mu\nu}+\overline{T}_{\mu\nu}), \tag{2}$$

with $F(R)\equiv\dfrac{df(R)}{dR}$, ∇_μ represents covariant differentiation, $T_{\mu\nu}$ serves as the standard matter energy momentum tensor whereas $\overline{T}_{\mu\nu}$ serves as energy momentum tensor associated with HDE.

Contraction of the field Equations (2) leads to

$$F(R)R-2f(R)+3\nabla^\mu\nabla_\mu F(R)=-(T+\overline{T}), \tag{3}$$

with $T = g_{\mu\nu}T^{\mu\nu}$ and $\overline{T} = g_{\mu\nu}\overline{T}^{\mu\nu}$. In a vacuum, the right-hand side of equation (3) vanishes, which gives us the relation between $f(R)$ and $F(R)$ as follows:

$$f(R) = \frac{1}{2}\left[3\nabla^{\mu}\nabla_{\mu}F(R) + F(R)R\right]. \tag{4}$$

Hypersurface-homogeneous models have been the subject of a significant amount of research, which can be described as

$$ds^2 = -dt^2 + A^2(t)dx^2 + B^2(t)\left[dy^2 + \Sigma^2(y,K)dz^2\right], \tag{5}$$

where A and B denotes the scale factors that depends on t only while $\Sigma(y,K) = \sin y, y, \sinh y$ with $K = 1, 0, -1$ respectively.

The corresponding scalar curvature R is

$$R = 2\left[\frac{\ddot{A}}{A} + 2\frac{\dot{A}\dot{B}}{AB} + 2\frac{\ddot{B}}{B} + \frac{\dot{B}^2}{B^2} + \frac{K}{B^2}\right], \tag{6}$$

where ' $\cdot$ ' denotes differentiation with respect to cosmic time t.

The energy momentum tensors are defined for both pressureless matter and HDE as

$$T_{\mu\nu} = \rho_m u_\mu u_\nu;\ \overline{T}_{\mu\nu} = (\rho_{de} + p_{de})u_\mu u_\nu + g_{\mu\nu}p_{de}, \tag{7}$$

where ρ_m serves as the energy density of matter, p_{de} and ρ_{de} are pressure and energy density of the HDE respectively while u_μ are component of the four-velocity vector of fluid satisfying $g_{\mu\nu}u^\mu u^\nu = -1$.

Using definition of EoS parameter (ω_{de}), the energy momentum tensors (7) can be written as

$$T_{\mu\nu} = \mathrm{diag}[0,0,0,-1]\rho_m;\ \overline{T}_{\mu\nu} = \mathrm{diag}[\omega_{de},\omega_{de},\omega_{de},-1]\rho_{de}. \tag{8}$$

And after parametrization, it reduces to

$$T_{\mu\nu} = \mathrm{diag}[0,0,0,-1]\rho_m;\ \overline{T}_{\mu\nu} = \mathrm{diag}[\omega_{de}+\gamma,\omega_{de},\omega_{de},-1]\rho_{de}. \tag{9}$$

within which the skewness parameter γ represents an offset from EoS parameter (ω_{de}) on x-direction.

Using equations (7)-(9), the field equations turn out to be

$$F\left[\frac{\ddot{A}}{A} + 2\frac{\ddot{B}}{B}\right] - \frac{1}{2}f(R) - \left(\frac{\dot{A}}{A} + 2\frac{\dot{B}}{B}\right)\dot{F} = \rho_m + \rho_{de}, \tag{10}$$

$$F\left[\frac{\ddot{A}}{A} + 2\frac{\dot{A}\dot{B}}{AB}\right] - \frac{1}{2}f(R) - 2\frac{\dot{B}}{B}\dot{F} - \ddot{F} = -(\omega_{de}+\gamma)\rho_{de}, \tag{11}$$

$$F\left[\frac{\ddot{B}}{B} + \frac{\dot{A}\dot{B}}{AB} + \frac{\dot{B}^2}{B^2} + \frac{K}{B^2}\right] - \frac{1}{2}f(R) - \left(\frac{\dot{A}}{A} + \frac{\dot{B}}{B}\right)\dot{F} - \ddot{F} = -\omega_{de}\rho_{de}. \tag{12}$$

Here, we have the HDE density in the form

$$\rho_{de} = 3\left(\alpha H^2 + \beta\dot{H}\right), \tag{13}$$

where H stands for the Hubble parameter while α, β serve as constants.

The above requisite was stated by Granda and Oliveros and requires compliance with constraints established according to the existing observational data. The directional Hubble parameters, indicating the rates of cosmic expansion alongside designated axes, are defined underneath as

$$H_x = \frac{\dot{A}}{A},\ H_y = \frac{\dot{B}}{B} = H_z. \tag{14}$$

The mean Hubble parameter is defined by

$$H=\frac{1}{3}\frac{\dot{V}}{V}=\frac{1}{3}\left(\frac{\dot{A}}{A}+2\frac{\dot{B}}{B}\right), \tag{15}$$

with $V = AB^2$ expressing the volume of the cosmos.
Using equations (14) and (15), the average anisotropy parameter turns out to be

$$\Delta=\frac{1}{3}\left(\frac{\Delta H_x+\Delta H_y+\Delta H_z}{H}\right)^2=\frac{2}{9H^2}\left(\frac{\dot{A}}{A}-\frac{\dot{B}}{B}\right)^2. \tag{16}$$

Using equations (11) and (12), we obtain

$$\frac{\dot{A}}{A}-\frac{\dot{B}}{B}=\frac{\lambda}{FV}+\frac{1}{FV}\int\left(\frac{KF}{B^2}-\gamma\rho_{de}\right)Vdt\,, \tag{17}$$

with λ denoting a constant of integration.
Consequently, the anisotropy parameter becomes

$$\Delta=\frac{2}{9H^2}\left[\frac{\lambda}{FV}+\frac{1}{FV}\int\left(\frac{KF}{B^2}-\gamma\rho_{de}\right)Vdt\right]^2. \tag{18}$$

By choosing $\gamma = 0$ in equation (18), we get isotropic case as

$$\Delta=\frac{2}{9H^2}\left[\frac{\lambda}{FV}+\frac{K}{FV}\int\frac{FV}{B^2}dt\right]^2. \tag{19}$$

The integral component in equation (18) is omitted with

$$\gamma=\frac{KF}{B^2\rho_{de}}. \tag{20}$$

Hence, the energy-momentum tensor (9) turns out to be

$$\overline{T}_{\mu\nu}=\mathrm{diag}\left[\omega_{de}+\frac{KF}{B^2\rho_{de}},\omega_{de},\omega_{de},-1\right]\rho_{de}, \tag{21}$$

whereas the anisotropy parameter (18) reduces to

$$\Delta=\frac{2\lambda^2}{9H^2F^2}V^{-2}. \tag{22}$$

3. SOLUTION TO FIELD EQUATIONS

Using equations (17) and (20), we obtain

$$\frac{A}{B}=c_1\exp\left(\lambda\int\frac{dt}{FV}\right), \tag{23}$$

where c_1 is integration constant.
Solving equation (23), we obtained the quadrature solutions associated with scale factors A and B described as

$$A=d_1a\exp\left[q_1\int\frac{dt}{Fa^3}\right], \tag{24}$$

and

$$B=d_2a\exp\left[q_2\int\frac{dt}{Fa^3}\right]. \tag{25}$$

Here $a=\left(AB^2\right)^{\frac{1}{3}}=V^{\frac{1}{3}}$ is average scale factor and $d_1=c_1^{\frac{2}{3}}$, $d_2=c_1^{-\frac{1}{3}}$, $q_1=\frac{2\lambda}{3}$, $q_2=-\frac{\lambda}{3}$, satisfying $d_1d_2^2=1$ and $q_1+2q_2=0$.

In order to solve the integral (24)-(25), we use the connection among the differential and scalar components of $f(R)$ as considered by Sharif and Shamir [36,37] given by

$$F = c_2 a^{-2}, \tag{26}$$

where c_2 is constant.

Using equations (24)-(26), we get

$$A = d_1 a \exp\left[\frac{q_1}{c_2}\int \frac{dt}{a}\right], \tag{27}$$

and

$$B = d_2 a \exp\left[\frac{q_2}{c_2}\int \frac{dt}{a}\right]. \tag{28}$$

We currently have three distinct equations involving seven unknown variables $A, B, \rho_m, \rho_{de}, \omega_{de}, \gamma$ and $f(R)$. Consequently, additional conditions are required to fully resolve the system. Additional conditions can be introduced through assumptions related to specific physical scenarios or arbitrary mathematical suppositions. Therefore, we assume three volumetric expansion laws expressed as

$$V = c_3 e^{3nt}, \tag{29}$$

$$V = c_4 t^{3m} \tag{30}$$

where c_3, c_4, n and m are positive constants.

4. EXPONENTIAL EXPANSION MODEL

The mean scale factor results in

$$a = k_1 e^{nt}, \tag{31}$$

where $k_1 = c_3^{1/3}$.

Using the established relation between scale factor $a(t)$ and redshift (z) as $a(t) = \frac{1}{1+z}$, we get the expression for cosmic time in relation to redshift for model (31) as follows

$$t(z) = -\frac{1}{n}\log\left[k_1(z+1)\right]. \tag{32}$$

Using equations (27), (28) and (31), the metric potentials are obtained as

$$A(z) = \frac{d_1}{1+z}\exp\left[\frac{2q_1}{nc_2}(1+z)\right]. \tag{33}$$

and

$$B(z) = \frac{d_2}{1+z}\exp\left[\frac{2q_2}{nc_2}(1+z)\right]. \tag{34}$$

Physical and Kinematical Properties

The directional Hubble Parameter are found to be

$$H_x = n + \frac{q_1}{c_2}(1+z);\ H_y = n + \frac{q_2}{c_2}(1+z) = H_z. \tag{35}$$

while the Mean Hubble Parameter turns out to be

$$H = n. \tag{36}$$

From equations (35)-(36), we noted that the H remains invariant, while the directional Hubble parameters fluctuate with time. The directional Hubble parameters approach to mean Hubble parameter as $t \to \infty$. The mean Hubble

parameter's derivative with regard to cosmic time being zero reveals the cosmos expanding at a rapid pace. Thus, it is possible to use the model that emerges to describe the dynamism of the late-time progression.

The deceleration parameter turns out to be

$$q = -1. \tag{37}$$

In accordance with recent studies of supernovae Ia , the negative value of q implies that universe appears to be expanding faster. Additionally, our findings align with the studies of Katore and Gore [19] and that of Rao and Neelima [44].

Scalar expansion and shear scalar are described respectively by

$$\theta = 3n\ , \tag{38}$$

and

$$\sigma^2 = \frac{q_1^2 + 2q_2^2}{2c_2^2}(1+z)^2\ . \tag{39}$$

The consistency of the exponential growth is indicated by the steady value of the expansion scalar θ. At the very beginning epoch, the shear scalar σ^2 reaches a constant value, while both parameters approach zero over extended periods of time. The ratio σ^2/θ^2 vanishes at sufficient large time indicating the universe's isotropic expansion which resemble with the work of Katore and Gore [19].

From equation (22), the mean anisotropic parameter turns out to be

$$\Delta = \frac{2\lambda^2}{9n^2c_2^2}(1+z)^2\ . \tag{40}$$

Using equations (13) and (36), the HDE density exhibits constant physical behaviour as it turns out to be

$$\rho_{de} = 3n^2\alpha. \tag{41}$$

Using equations (20), (26), (33) and (41), the Skewness parameter is obtained as

$$\gamma = \frac{Kc_2}{3\alpha n^2 d_2^2}(1+z)^4 \exp\left[\frac{2q_2}{nc_2}(1+z)\right]. \tag{42}$$

From equations (6) and (33), the Ricci scalar is obtained as

$$R = 2\left\{6n^2 + \frac{K}{d_2^2}(1+z)^2 \exp\left[\frac{2q_2}{nc_2}(1+z)\right] + \frac{3q_2^2}{c_2^2}(1+z)^2\right\}. \tag{43}$$

and the scalar function $f(R)$ is given by equation (4)

$$f(R) = \left\{\frac{9n^2}{(1+z)^2} + \frac{K}{d_2^2}\exp\left[\frac{2q_2}{nc_2}(1+z)\right]\right\}c_2(1+z)^4 + 3c_2^{-1}q_2^2(1+z)^4\ . \tag{44}$$

The matter energy density is

$$\rho_m = \frac{c_2}{2}(1+z)^2\left\{9n^2 - \frac{K}{d_2^2}(1+z)^2 \exp\left[\frac{2q_2}{nc_2}(1+z)\right]\right\} + \frac{(q_1-q_2)^2}{2c_2}(1+z)^4 - 3n^2\alpha. \tag{45}$$

The EoS parameter is given by

$$\omega_{de} = \frac{(1+z)^4}{6n^2\alpha c_2 d_2^2}\left\{d_2^2\left(\frac{3n^2c_2^2}{(1+z)^2} + q_1^2 - q_2^2\right) - Kc_2^2 \exp\left[\frac{2q_2}{nc_2}(1+z)\right]\right\} \tag{46}$$

Dark energy pressure is found to be

$$p_{de} = \frac{c_2(1+z)^4}{2}\left\{\frac{3n^2}{(1+z)^2} - \frac{K}{d_2^2}\exp\left[\frac{2q_2}{nc_2}(1+z)\right]\right\} + \frac{(q_1^2 - q_2^2)}{2c_2}(1+z)^4\ . \tag{47}$$

Overall density is given by

$$\Omega = \frac{c_2 (1+z)^4}{6n^2}\left\{\frac{9n^2}{(1+z)^2} - \frac{K}{d_2^2}\exp\left[\frac{2q_2}{nc_2}(1+z)\right] + c_2^{-2}(q_1 - q_2)^2\right\}. \tag{48}$$

Now we obtain the graphical representation of these parameters against redshift for three cases of $K = 1, 0, -1$ by taking appropriate choices of various constants involved in it. We take $d_2 = 0.1$, $\alpha = 5$, $c_2 = 1$, $k_1 = 1$, $q_1 = 2/3$, and $q_2 = -1/3$, with $\lambda = 1$, and from equation (36), we take $n = 67$ with reference to the current Hubble parameter value $H_0 = 67.4 \pm 0.5$ $kms^{-1}Mpc^{-1}$ by the Planck 2018 results [45], assuming the standard ΛCDM cosmology.

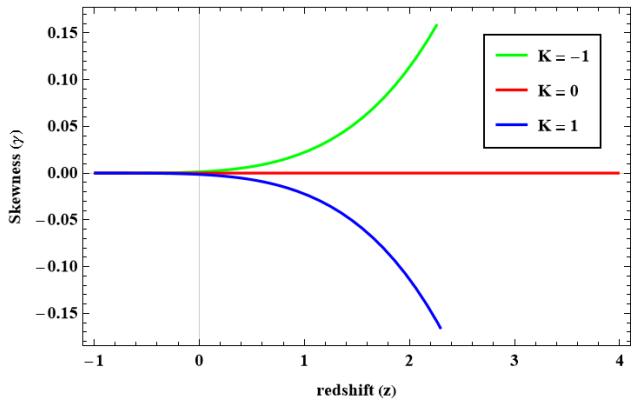

Figure 1. Plot of skewness parameter (γ) versus redshift (z).

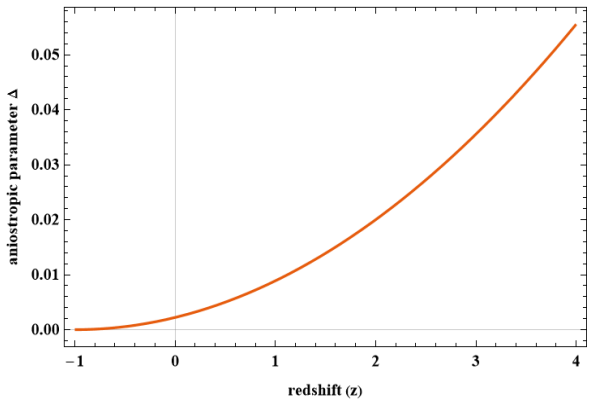

Figure 2. Plot of anisotropic parameter (Δ) versus redshift (z).

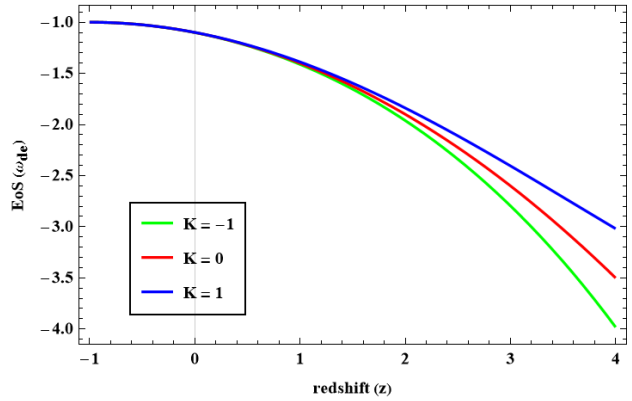

Figure 3. Plot of EoS parameter (ω_{de}) versus redshift (z)

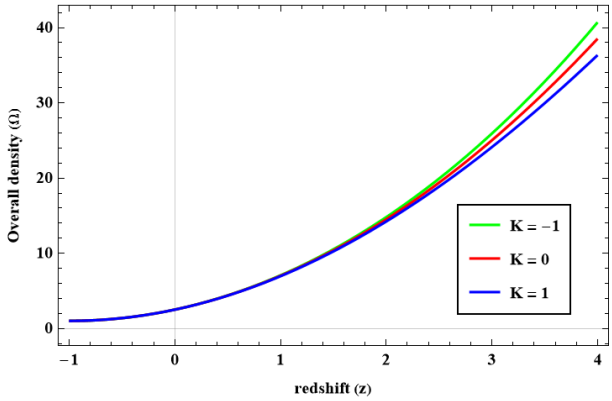

Figure 4. Plot of overall density (Ω) versus redshift (z)

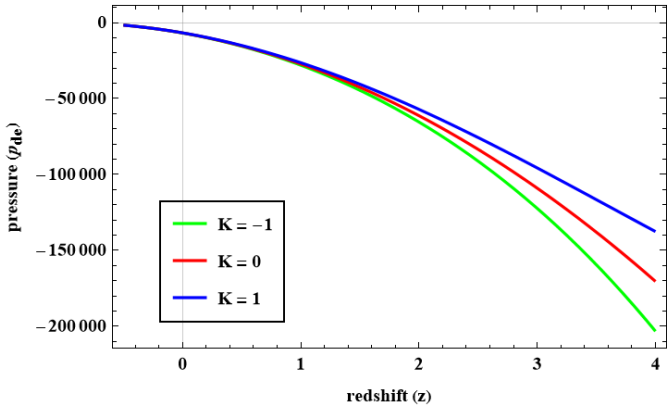

Figure 5. Plot of pressure (p) versus redshift (z)

From Figs. 1 and 2, the skewness parameter and anisotropic parameter indicate isotropisation of the universe as similar to the case of the hybrid model. The graphical representation in Fig. 3 depicts the variation of the EoS parameter during the progression of redshift. In the past, the behaviour of $\omega_{de} < -1$ shows the dominance by phantom energy. However, in the near future, $\omega_{de} \to -1$ predicts the ΛCDM model. The progression of the overall density parameter

against redshift is illustrated in Fig. 4. As cosmic development progresses, the overall density parameter diminishes, and for a proper choice of the constants, it approaches 1, indicating the flat universe that agrees with evidence from observations of the cosmos, whereas matter energy density follows the increasing behaviour as $z \to \infty$. Fig. 5 displays the approach of pressure against redshift, which shows that the resulting model is accelerating due to an ongoing presence of negative pressure, which is in accordance with the findings underlined in [46].

5. POWER EXPANSION MODEL

The mean scale factor results in

$$a = k_3 t^m, \tag{49}$$

where $k_3 = c_5^{1/3}$.

The relation for cosmic time and redshift for model (49) is found to be

$$t(z) = \left[k_2 (z+1)\right]^{-1/m}. \tag{50}$$

Using equations (27)-(28) and (49)-(50), the prospective metrics potentials in redshift are obtained as

$$A(z) = \frac{d_1}{1+z} \exp\left[-\frac{(1+z)q_1}{(m-1)c_2}\left((1+z)k_2\right)^{-1/m}\right], \tag{51}$$

and

$$B(z) = \frac{d_1}{1+z} \exp\left[-\frac{(1+z)q_2}{(m-1)c_2}\left((1+z)k_2\right)^{-1/m}\right]. \tag{52}$$

The Ricci scalar is

$$R = 6m(2m-1)\left(k_2(1+z)\right)^{2/m} + 2(1+z)^2\left\{\frac{K}{d_2^2}\exp\left[\frac{2q_2(1+z)}{(m-1)c_2}\left((1+z)k_2\right)^{-1/m}\right] + \frac{3q_2^2}{c_2^2}\right\} \tag{53}$$

PHYSICAL AND KINEMATICAL PROPERTIES

The directional Hubble parameters can be expressed as

$$H_x = m\left[k_2(z+1)\right]^{1/m} + \frac{q_1}{c_2}(1+z);\ H_y = m\left[k_2(z+1)\right]^{1/m} + \frac{q_2}{c_2}(1+z) = H_z. \tag{54}$$

and mean Hubble parameter turns out to be

$$H = m\left[k_2(z+1)\right]^{1/m}. \tag{55}$$

The deceleration parameter turns out to be

$$q = \frac{1}{m} - 1. \tag{56}$$

For $m < 1$, it indicates a decelerating cosmos as $q > 0,$ whereas for $m > 1$, it describes rapid expansion of the cosmos as $q < 0$, that is in line with the studies of Sarkar and Mahanta [47].

The scalar expansion, shear scalar and mean anisotropic parameter are expressed respectively by

$$\theta = 3H = 3m\left[k_2(z+1)\right]^{1/m} \tag{57}$$

$$\sigma^2 = \frac{q_1^2 + 2q_2^2}{2c_2^2}(1+z)^2. \tag{58}$$

and

$$\Delta = \frac{2\lambda^2}{9m^2c_2^2}(1+z)^2\left[k_2(1+z)\right]^{-2/m} \tag{59}$$

The HDE density is

$$\rho_{de} = 3m(m\alpha - \beta)\left[k_2(1+z)\right]^{2/m} \tag{60}$$

Skewness parameter is found to be

$$\gamma=\frac{Kc_2(1+z)^4\left((1+z)k_2\right)^{-2/m}}{3m(m\alpha-\beta)d_2^2}\exp\left[-\frac{(1+z)q_2}{(m-1)c_2}\left((1+z)k_2\right)^{-1/m}\right]. \tag{61}$$

From equation (6), the Ricci scalar is obtained as

$$R=6m(2m-1)\left(k_2(1+z)\right)^{2/m}+2(1+z)^2\left\{\frac{K}{d_2^2}\exp\left[\frac{2q_2(1+z)}{(m-1)c_2}\left(k_2(1+z)\right)^{-1/m}\right]+\frac{3q_2^2}{c_2^2}\right\}. \tag{62}$$

and the scalar function $f(R)$ is given by equation (4)

$$f(R)=\frac{(1+z)^4}{c_2}\left\{\frac{3m(3m-2)}{(1+z)^2}\left((1+z)k_2\right)^{2/m}+c_2^2\left(\frac{K}{d_2^2}\exp\left[\frac{2q_2(1+z)}{(m-1)c_2}\left(k_2(1+z)\right)^{-1/m}\right]\right)+3q_2^2\right\}. \tag{63}$$

The matter density is

$$\begin{aligned}\rho_m=&\frac{c_2(1+z)^4}{2}\left\{\frac{9m^2\left((1+z)k_2\right)^{2/m}}{(1+z)^2}-\frac{K}{d_2^2}\exp\left[\frac{2(1+z)q_2}{(m-1)c_2}\left(k_2(1+z)\right)^{-1/m}\right]\right\}\\&+3m(\beta-m\alpha)\left(k_2(1+z)\right)^{2/m}+\frac{(q_1-q_2)^2}{2c_2}(1+z)^4.\end{aligned} \tag{64}$$

The EoS parameter is given by

$$\omega_{de}=\frac{(1+z)^4}{6m(m\alpha-\beta)c_2}\left\{\frac{3m^2c_2^2}{(1+z)^2}+\frac{\left((1+z)k_2\right)^{-2/m}}{d_2^2}\left(-Kc_2^2\exp\left[\frac{2q(1+z)_2}{(m-1)c_2}\left(k_2(1+z)\right)^{-1/m}\right]+d_2^2\left(q_1^2-q_2^2\right)\right)\right\}. \tag{65}$$

Dark energy pressure is obtained as

$$p_{de}=\frac{(1+z)^4}{2c_2d_2^2}\left\{-c_2^2K\exp\left[\frac{2q(1+z)_2}{(m-1)c_2}\left(k_2(1+z)\right)^{-1/m}\right]+\frac{3m^2d_2^2c_2^2}{(1+z)^2}\left((1+z)k_2\right)^{2/m}+d_2^2\left(q_1^2-q_2^2\right)\right\}. \tag{66}$$

Overall density is found to be

$$\Omega=\frac{(1+z)^4}{6m^2c_2d_2^2}\left((1+z)k_2\right)^{-2/m}\left\{\frac{9m^2d_2^2c_2^2}{(1+z)^2}\left(k_2(1+z)\right)^{2/m}-c_2^2K\exp\left[\frac{2q(1+z)_2}{(m-1)c_2}\left(k_2(1+z)\right)^{-1/m}\right]+d_2^2(q_1-q_2)^2\right\}. \tag{67}$$

Now, the graphical representation of these parameters against redshift for three cases of $K=1,0,-1$ are obtained by taking appropriate choices of various constants involved in it. We consider $d_2=0.1$, $\alpha=5,\beta=1$ $c_2=1$, $k_2=1$, $q_1=2/3$, $q_2=-1/3$, with $\lambda=1$, and from equation (55), we take $m=67$ with reference to the $H_0=67.4\pm0.5$ $kms^{-1}Mpc^{-1}$ estimated in the Planck 2018 results [45].

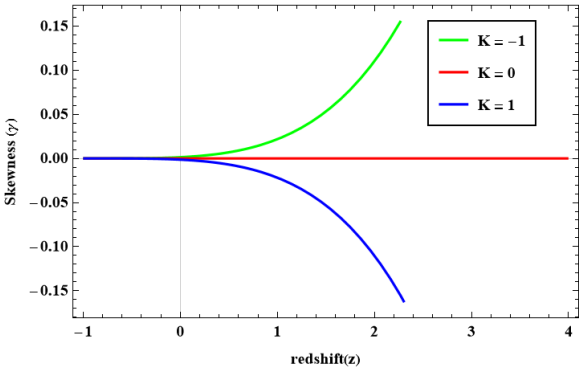

Figure 6. Plot of skewness parameter (γ) versus redshift (z)

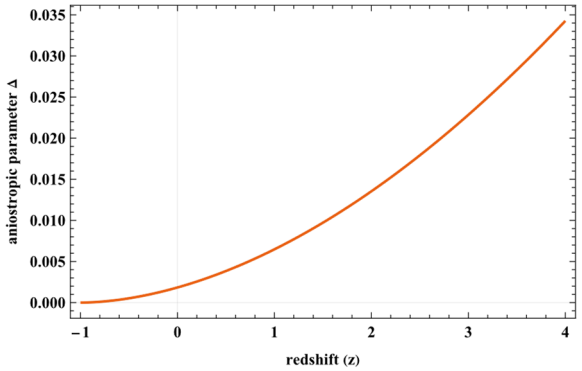

Figure 7. Plot of anisotropic parameter (Δ) versus redshift (z)

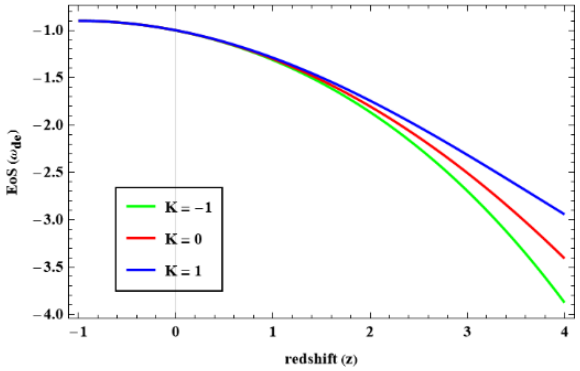

Figure 8. Plot of EoS (ω_{de}) versus redshift (z)

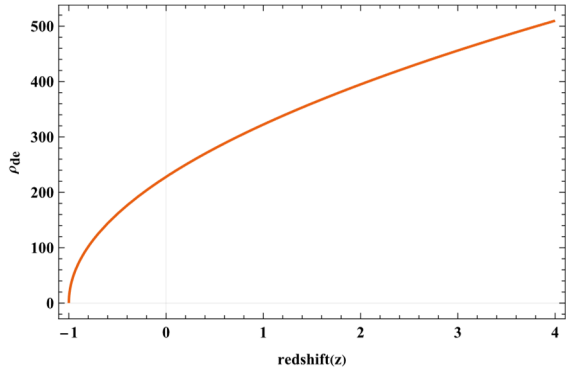

Figure 9. Plot of HDE density (ρ_{de}) versus redshift (z)

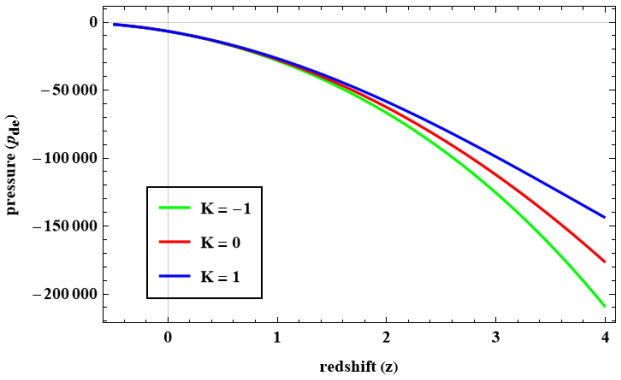

Figure 10. Approach of pressure (p_{de}) against redshift (z)

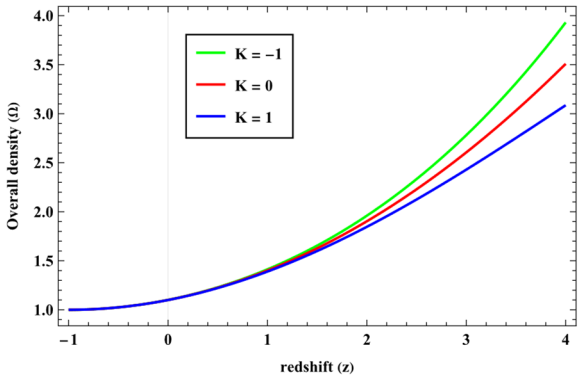

Figure 11. Plot of overall density (Ω) versus redshift (z)

Late-time isotropisation of the cosmos is reflected through the demonstration in Fig. 6 and Fig. 7 as the skewness parameter and anisotropic parameter become zero at $z \to -1$. From Fig. 8, the EoS parameter initially starts with a positive value and reaches to $\omega_{de} = -1$ at $z \to -1$ indicating the model in the future. The evolution of HDE density is displayed in Fig. 9, which indicates its declining nature while avoiding fine-tuning. The negative value of pressure with the evolution of redshift is illustrated in Fig. 10, indicating that the expansion of the cosmos is accelerating, while Fig. 11 displays the progression of the overall density parameter against redshift with $\Omega \to 1$ at $z \to -1$ specifying a flat cosmos.

6. STATEFINDER DIAGNOSTIC AND STABILITY ANALYSIS OF MODELS

6.1 Statefinder Diagnostics of Models

The statefinder diagnostic as proposed by Sahni et al. [54], serves as a proficient tool for differentiating among various cosmological models. Its definition is

$$r \equiv \frac{\dddot{a}}{aH^3} \text{ and } s \equiv \frac{r-1}{3(q-1/2)}. \tag{68}$$

6.1.1 For exponential expansion model

From equations (31), (36)-(37), statefinder parameters pair (68) for exponential expansion model reduces to $\{r,s\} \to \{1,0\}$ representing the ΛCDM model and resembles with the investigations of Katore and Gore [19] and Samanta [46].

6.1.2 For power expansion model

The statefinder parameters (68) for power expansion model turn out to be

$$r = \frac{(m-1)(m-2)}{m^2} \text{ and } s = \frac{2}{3m}. \tag{69}$$

And their association is found to be

$$r = 1 + \frac{9}{2}s(s-1). \tag{70}$$

The visualization of r against s is displayed in Fig. 12. Its route goes through the DE region of Chaplygin Gas (CG) and quintessence [56] in the $r-s$ plane and tends to approach the ΛCDM model in the near future, which resemble with the findings discussed in [57].

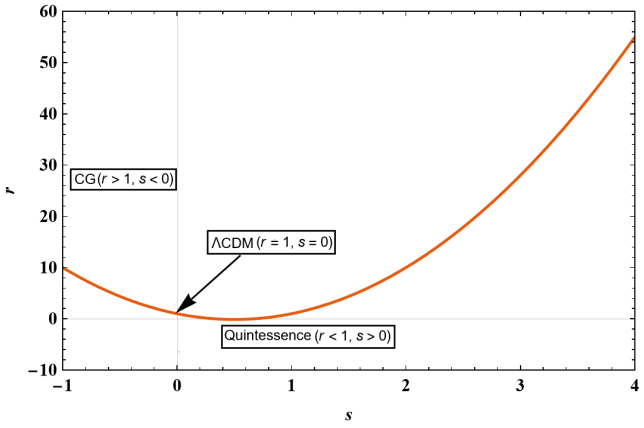

Figure 12. Plot of r versus s (Power expansion model)

6.2 STABILITY ANALYSIS OF MODEL

The model's stability is evaluated through the examination of the parameter identified as the squared speed of sound v_s^2 as proposed by Sadeghi et al. [58]. If the value of v_s^2 is positive, model exhibits stability whereas for a negative value of v_s^2, the model is unstable. It is specified by

$$v_s^2 = \frac{dp_{de}}{d\rho_{de}}. \tag{71}$$

Using equations (66) and (66), the stability parameter (71) for power expansion model is found to be

$$v_s^2 = \frac{(1+z)^5}{6m(m\alpha-\beta)c_2d_2^2}\times\left\{\begin{array}{l}\dfrac{3m^2c_2^2d_2^2}{(1+z)^3}(m+1)-Kc_2q_2\left[k_2(1+z)\right]^{-3/m}\exp\left[\dfrac{2q_2(1+z)}{(m-1)c_2}\left((1+z)k_2\right)^{-1/m}\right] \\ -\dfrac{2m\left[k_2(1+z)\right]^{-2/m}}{1+z}\left[Kc_2^2\exp\left[\dfrac{2q_2(1+z)}{(m-1)c_2}\left((1+z)k_2\right)^{-1/m}\right]+d_2^2\left(q_2^2-q_1^2\right)\right]\end{array}\right\}. \tag{72}$$

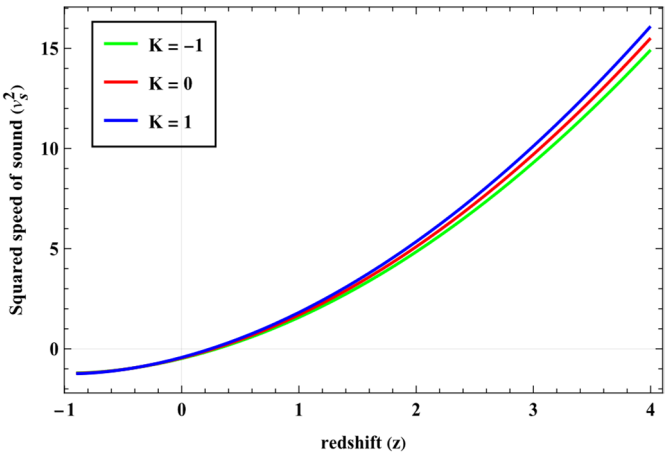

Figure 13. Inspection of squared speed of sound (v_s^2) against redshift (z)

Fig. 13 illustrates the variations in the squared speed of sound (v_s^2) against redshift (z). We noticed that $v_s^2 > 0$ for all the positive values of redshift (z), indicating its stability up to the present time, but $v_s^2 < 0$ for the negative domain indicating the model's instability in the future.

7. CONCLUSIONS

This paper examined the behaviour of HDE in $f(R)$ gravity across a hypersurface-homogeneous spacetime, focusing on exponential and power-law expansions. Here is a brief overview of our study's findings:

- The exponential expansion model yields a constant Hubble parameter while $q=-1$ indicating sustained accelerated expansion and an EoS transitioning from phantom-like ($\omega_{de}<-1$) to ΛCDM ($\omega_{de}\to-1$), aligning with late-time acceleration.
- The power-law model shows deceleration-to-acceleration behaviour ($q>0$ and $q<0$) depending on $m<1$ and $m>1$ respectively, with the EoS parameter evolving from quintessence to ΛCDM.
- Both models exhibit complete late-time isotropisation $(\Delta,\ \gamma\to0)$, consistent with CMB observations that suggest large-scale homogeneity.
- The statefinder diagnostic distinguishes the evolutionary paths of the two models: the exponential model closely tracks the ΛCDM trajectory, while the power-law model passes through the quintessence and phantom regimes before covering ΛCDM.
- We have done some stability tests, and it looks like the exponential solution is the most stable throughout cosmic evolution, whereas the power-law model shows late-time instabilities.
- The HDE density shows a declining nature while avoiding fine-tuning, and the overall density parameter is maintaining $\Omega\to1$ for a flat cosmos.
- The present framework successfully unifies inflation and contemporary cosmic acceleration, with residual anisotropic effects providing a potential window into early-universe dynamics.

This work links quantum gravity principles with cosmology, making testable predictions for future research and showing that HDE is a viable alternative to ΛCDM.

Acknowledgments

The authors express their sincere gratitude to the editor and the anonymous reviewer(s) for their valuable comments and constructive suggestions, which significantly improved the quality and clarity of the manuscript.

ORCID

A.Y. Shaikh, https://orcid.org/0000-0001-5315-559X; **A.P. Jenekar**, https://orcid.org/0009-0005-8928-3725

REFERENCES

[1] A.G. Riess, *et al.*, Astron. J. **116**, 1009 1998). https://doi.org/10.1086/300499
[2] A.G. Riess, *et al.*, Astron. J. **117**, 707 (1999). https://doi.org/10.1086/300738
[3] S. Perlmutter, *et al.*, Astrophys. J. **517**, 565 (1999). https://doi.org/10.1086/307221
[4] P. De Bernardis, *et al*., Nature, **404**, (2000). https://doi.org/10.1038/35010035
[5] E. Komatsu, *et al.*, Astrophys. J. Suppl. Ser. **192**, 18 (2011). http://dx.doi.org/10.1088/0067-0049/180/2/330
[6] M. Tegmark, *et al.*, Phys. Rev. D, **69**, 103501 (2004). https://doi.org/10.1103/PhysRevD.69.103501
[7] U. Seljak, *et al.*, Phys. Rev. D, **71**, 103515 (2005). https://doi.org/10.1103/PhysRevD.71.103515
[8] K. Bamba, *et al.*, Astrophys. Space Sci. **342**, 155 (2012). https://doi.org/10.1007/s10509-012-1181-8
[9] M. Sharif and M. Zubair, Astrophys. Space Sci. **330**, 399 (2010). https://doi.org/10.1007/s10509-010-0414-y
[10] S.M. Carroll, W.H. Press, and E.L. Turner, Annu. Rev. Astron. Astrophys. **30**, 499 (1992). https://doi.org/10.1146/annurev.aa.30.090192.002435
[11] M.S. Turner, and M. White, Phys. Rev. D, **56**, R4439 (1997). https://doi.org/10.1103/PhysRevD.56.R4439
[12] V. Sahni, and L. Wang, Phys. Rev. D, **62**, 103517 (2000). https://doi.org/10.1103/PhysRevD.62.103517
[13] A.G. Cohen, D.B. Kaplan, and A.E. Nelson, Phys. Rev. Lett. **82**, 4971 (1999). https://doi.org/10.1103/PhysRevLett.82.4971
[14] M. Li, Physics Letters B, **603**, 1-2 (2004). https://doi.org/10.1016/j.physletb.2004.10.014
[15] V.C. Dubey, and U.K. Sharma, New Astron. **86**, 101586 (2021). https://doi.org/10.1016/j.newast.2021.101586
[16] S. Capozziello, P. Martin-Moruno, and C. Rubano, Phys. Lett. B, **664**, 12 (2008). https://doi.org/10.1016/j.physletb.2008.04.061
[17] S. Nojiri, and S. D. Odintsov, Phys. Lett. B, **659**, 821 (2008). https://doi.org/10.1016/j.physletb.2007.12.001
[18] D.D. Pawar, R.V. Mapari, and P.K. Agrawal, J. Astrophys. Astron. **40**, 13 (2019). https://doi.org/10.1007/s12036-019-9582-5
[19] S.D. Katore, and S.V. Gore, J. Astrophys. Astron. **41**, 12 (2020). https://doi.org/10.1007/s12036-020-09632-z
[20] C.P. Singh, and A. Beesham, Gravit. Cosmol. **17**, 284 (2011). https://doi.org/10.1134/S020228931103008X
[21] H.A. Buchdahl, Mon. Not. R. Astron. Soc. **150**, 1 (1970). https://doi.org/10.1093/mnras/150.1.1
[22] A.A. Starobinsky, JETP Lett. **86**, 157 (2007). https://doi.org/10.1134/S0021364007150027
[23] P.A.R. Ade, *et al.*, A&A, **571**, A22 (2014). https://doi.org/10.1051/0004-6361/201321569
[24] S.D. Katore, and A.Y. Shaikh, Astrophys. Space Sci. **357**, 27 (2015). https://doi.org/10.1007/s10509-015-2297-4
[25] S.H. Shekh, and K. Ghaderi, Phys. Dark Universe **31**, 100785 (2021). https://doi.org/10.1016/j.dark.2021.100785
[26] T. Vinutha, K.V. Vasavi, and K.S. Kavya, Int. J. Geom. Methods Mod. Phys. **20**, 2350119 (2023). https://doi.org/10.1142/S0219887823501190
[27] L.N. Granda, and A. Oliveros, Phys. Lett. B, **669**, 275 (2008). https://doi.org/10.1016/j.physletb.2008.10.017
[28] S. Kumar, and C.P. Singh, Astrophys. Space Sci. **312**, 57 (2007). https://doi.org/10.1007/s10509-007-9623-4
[29] C.P. Singh, S. Ram, and M. Zeyauddin, Astrophys. Space Sci. **315**, 181 (2008). https://doi.org/10.1007/s10509-008-9811-x
[30] J.P. Singh, and P.S. Baghel, Int. J. Theor. Phys. **48**, 449 (2009). https://doi.org/10.1007/s10773-008-9820-0

[31] Ö. Akarsu, and C.B. Kılınç, Gen. Relativ. Gravit. **42**, 119 (2009). https://doi.org/10.1007/s10714-009-0821-y
[32] Ö. Akarsu, and C.B. Kılınç, Gen. Relativ. Gravit. **42**, 763 (2010). https://doi.org/10.1007/s10714-009-0878-7
[33] K.S. Adhav, *et al.*, Astrophys. Space Sci. **332**, 497 (2011). https://doi.org/10.1007/s10509-010-0519-3
[34] V.B. Johri, and K. Desikan, Gen. Relativ. Gravit. **26**, 1217 (1994). https://doi.org/10.1007/BF02106714
[35] K. Uddin, J.E. Lidsey, and R. Tavakol, Class. Quantum Gravity, **24**, 3951 (2007). https://doi.org/10.1088/0264-9381/24/15/012
[36] M. Sharif and M.F. Shamir, Class. Quantum Gravity, **26**, 235020 (2009). https://doi.org//10.1088/0264-9381/26/23/235020
[37] M. Sharif and M.F. Shamir, Mod. Phys. Lett. A, **25**, 1281 (2010). https://doi.org/10.1142/S0217732310032536
[38] S.D. Katore, *et al.*, Commun. Theor. Phys. **62**, 768 (2014). https://doi.org/10.1088/0253-6102/62/5/21
[39] Y. Younesizadeh, and A. Rezaie, Int. J. Mod. Phys. A, **37**, 2250040 (2022). https://doi.org/10.1142/S0217751X22500403
[40] V. Sahni, *et al*., J. Phys. Lett. 77, 201-206 (2003). https://doi.org/10.1134/1.1574831
[41] L. Perivolaropoulos and F. Skara, New Astron. Rev. **95**, 101659 (2022). https://doi.org/10.1016/j.newar.2022.101659
[42] P.A.R. Ade, *et al.*, Astron. Astrophys. **571**, A16 (2014). https://doi.org/10.1051/0004-6361/201525830
[43] R.A. Knop, *et al.*, Astrophys. J. **598**, 102 (2003). https://doi.org/10.1086/378560
[44] V.U.M. Rao, and D. Neelima, Eur. Phys. J. Plus, **128**, 35 (2013). https://doi.org/10.1140/epjp/i2013-13035-y
[45] Planck Collaboration, *et al*., Astron. Astrophys. **641**, A6 (2020). https://doi.org/10.1051/0004-6361/201833910
[46] G.C. Samanta, Int. J. Theor. Phys. **52**, 4389 (2013). https://doi.org/10.1007/s10773-013-1757-2
[47] S. Sarkar, and C.R. Mahanta, Int. J. Theor. Phys. **52**, 1482 (2013). https://doi.org/10.1007/s10773-012-1468-0
[48] C. Zhang, *et al.*, Res. Astron. Astrophys. **14**, 1221 (2014). https://doi.org/10.1088/1674-4527/14/10/002
[49] J. Simon, L. Verde, and R. Jimenez, Phys. Rev. D, **71**, 123001 (2005). https://doi.org/10.1103/PhysRevD.71.123001
[50] M. Moresco, *et al.*, J. Cosmol. Astropart. Phys. 006 (2012). https://doi.org/10.1088/1475-7516/2012/08/006
[51] M. Moresco, *et al.*, J. Cosmol. Astropart. Phys. 014 (2016). https://dx.doi.org/10.1088/1475-7516/2016/05/014
[52] A.L. Ratsimbazafy, *et al.*, Mon. Not. R. Astron. Soc. **467**, 3239 (2017). https://doi.org/10.1093/mnras/stx301
[53] S. Capozziello, S. Nojiri, and S. D. Odintsov, Phys. Lett. B, **781**, 99 (2018). https://doi.org/10.1016/j.physletb.2018.03.064
[54] V. Sahni, *et al.*, J. Exp. Theor. Phys. Lett. **77**, 201 (2003). https://doi.org/10.1134/1.1574831
[55] U. Alam, *et al.*, Mon. Not. R. Astron. Soc. **344**, 1057 (2003). https://doi.org/10.1103/PhysRevD.68.127501
[56] Y.B. Wu, *et al.*, Gen. Relativ. Gravit. **39**, 653 (2007). https://doi.org/10.1007/s10714-007-0412-8
[57] A.Y. Shaikh, Eur. Phys. J. Plus, **138**, 301 (2023). https://doi.org/10.1140/epjp/s13360-023-03931-4
[58] J. Sadeghi, A.R. Amani, and N. Tahmasbi, Astrophys. Space Sci. **348**, 559 (2013). https://doi.org/10.1007/s10509-013-1579-y

ОБМЕЖЕНА ДИНАМІКА ГОЛОГРАФІЧНОЇ ТЕМНОЇ ЕНЕРГІЇ В МОДИФІКОВАНІЙ f(R) ГРАВІТАЦІЇ

А.Й. Шейх[a], А.П. Дженекар[b], С.М. Шінгне[c]
[a]Кафедра математики, Індіра Ганді Кала Махавідьялая, Ралегаон-445402, M.S., Індія
[b]Кафедра математики, мистецтв, комерції та науки Коледж, Марегаон-445303, M.S., Індія
[c]Кафедра математики, Коледж наук, мистецтв та комерції ім. Г.С., Кхамгаон-444312, M.S., Індія

У цій роботі ми досліджуємо динамічну поведінку голографічної темної енергії (ГТЕ) в рамках модифікованої *f*(*R*) гравітації в однорідному гіперповерхневому просторі-часі. Щоб дослідити еволюційну поведінку Всесвіту під впливом темної енергії, ми розглядаємо як експоненціальні, так і степеневі розклади. Космічну еволюцію проаналізовано за допомогою стандартної космологічної діагностики, включаючи параметр густини та параметр рівняння стану (EoS) разом із параметром уповільнення. Крім того, діагностична пара statefinder тестується для точного виявлення різних фаз Всесвіту. Параметр квадрата швидкості звуку був використаний для включення аналізу стабільності до наших моделей. Це дослідження пов'язує принципи квантової гравітації з космологією, створюючи перевірені прогнози для майбутніх досліджень та ілюструючи, що HDE функціонує як надійна альтернатива ΛCDM.

Ключові слова: *гіперповерхнево-однорідний простір-час; f(R) гравітація; голографічна темна енергія*